UDK 621.791.3:62-426:539.55
Izvirni znanstveni članek

ISSN 1580-2949
MTAEC9, 39(5)155(2005)

GEOMETRICAL MODELS FOR THE DEFORMATION OF ROUND REINFORCEMENT WIRES WHEN COMPRESSING A REINFORCED BRAZED JOINT

GEOMETRIJSKI MODELI DEFORMACIJE OKROGLIH ŽIC ARMATURE PRI STISKANJU ARMIRANEGA SPAJKANEGA SPOJA

Borut Zorc[1], Ladislav Kosec[2]

[1]Welding Institute, Ptujska 19, 1000 Ljubljana, Slovenia
[2]Faculty of Natural Science and Technology, Aškerčeva c. 12, 1000 Ljubljana, Slovenia
agnes.brezovnik@guest.arnes.si

Prejem rokopisa – received: 2004-09-25; sprejem za objavo – accepted for publication: 2005-07-05

A reinforcement that coalesces with the parent metal will considerably improve the toughness, strength, and crack resistance of a brazed joint. Coalescence in a large area is obtained by the application of compression to test pieces during brazing, which results in deformation of round reinforcement wires into flat profiles. Various theoretical geometrical models of wire flattening that might be applicable for an advance estimate of the width of the coalescence between the reinforcement wires and the parent metal are shown and analysed for comparison.

Keywords: brazed joint, reinforcement, wire deformation

Armatura, ki se je zrasla z osnovnim materialom, občutno poveča žilavost, trdnost in odpornost proti razpokanju spajkanega spoja. Zraščanje na veliki površini dosežemo s stiskanjem vzorcev med spajkanjem. To ima za posledico deformacijo žic armature v ploske profile. Prikazani in primerjalno analizirani so različni teoretični geometrijski modeli sploščenja žice, kar se lahko uporabi za vnaprejšnjo oceno širine zraščenja armaturnih žic z osnovnim materialom.

Ključne besede: spajkan spoj, armatura, deformacija žice

1 INTRODUCTION

Reinforcements in the form of a plate, a mesh, fibres, and particles are added to a brazed joint in order to compensate for the thermal stresses in ceramics/metal joints, which are a result of different thermal extensions of the materials brazed [1-3]. Similar composite joints can also be produced by diffusion welding or solid-state bonding [4,5].

As a rule none of the hitherto known methods of reinforcement of a brazing joint eliminates its characteristic imperfections, i.e., low toughness and low resistance to crack initiation and propagation. This is a result of the absence of coalescence of the reinforcement and the parent metal. External loads are transmitted to the reinforcement through the brazing metal; therefore, the reinforcement plays no active role in the joint. The joint properties are determined by the brazing metal and its coalescence with the parent metal. The joint thus reinforced will mainly improve the shear strength, but not the other types of strength. In this case the brazing metal is distributed in the same way as in conventional brazed joints, i. e., across the total joint plane. Thus, it can be concluded that the mechanical properties of the brazed joint depend on the brazing-metal distribution. If the brazing metal, however, is prevented from distributing continuously across the joint plane, and a strong and tough connection with the parent metal is made to form at barrier locations, the imperfections of the brazed joint can be eliminated.

On the basis of the above findings a reinforced brazed joint with a reinforcement consisting of parallel wires with a round cross-section (comb system) has been developed [6]. Such a reinforcement eliminates all the imperfections of the brazed joint in metal materials simultaneously, provided that it has coalesced with the parent metal. Because of a different distribution, the brazing metal cannot affect the joint properties decisively. They are now dependent on the width of coalescence c_n of an individual reinforcement wire with the parent metal (**Figure 1**): the greater the width, the better the mechanical properties of the joint. Thus, the toughness properties of common brazed joints on low-carbon and austenitic steels brazed with silver brazing filler metal, L-Ag40Cd (DIN 8513), will improve from 10 J/cm^2 to as high as 150 J/cm^2 if the inserted steel-wire reinforcement coalesces with the parent metal. The carrier of the mechanical properties of the joint will now be the reinforcement and not the brazing metal, which makes the reinforcement play an active role in the transmission of loads across the joint. This, however, was not a characteristic of the brazed joints known till now.

The coalescence between the reinforcement and the parent metal occurs in the molten pool during diffusion brazing, in which case the brazing-metal eutectic

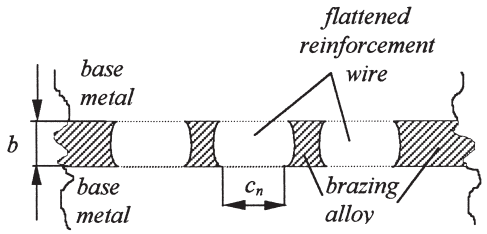

Figure 1: Scheme of a reinforced, brazed joint with a coalesced reinforcement of parallel flattened wires with a round cross-section
Slika 1: Shema armiranega spajkanega spoja z zraščeno armaturo iz vzporednih sploščenih žic s prvotno okroglim presekom

transforms into the solid solution. The process is controlled by diffusion, e. g., of phosphorus from the nickel-base brazing metal BNi-7 (**Figure 2A**) or copper-base brazing metal BCuP-2 (**Figure 2B**) into the parent metal and the reinforcement. In diffusion brazing, the brazing metal plays an active role in the solid and tough coalescence between the reinforcement and the parent metal. Another way of coalescing the two is by means of solid diffusion welding. In this case the brazing metal does not participate in the coalescence between the reinforcement and the parent metal. It is vital to remove the brazing metal from the coalescence location, which may be achieved by compressing the test pieces. This process is controlled by diffusion between the reinforcement and the parent metal and the processes of recrystallisation and growth of the crystal grains beyond the contact surface between the reinforcement and the parent metal. An example of this is the brazing of steel with a silver brazing metal and a steel reinforcement (**Figure 2C**).

In order to obtain the required width of the coalescence between the reinforcement and the parent metal, the test pieces should be compressed during brazing so that the wires concerned will flatten or get impressed into the parent metal. If the reinforcement is more ductile, i. e., deformable, than the parent metal, the wires will flatten with a negligible impression into the parent metal (**Figure 2**). The state of the flattened wires in the joint is similar to that in the solid bonding of ceramics or glass with a wire or a wire ring [7,8], where the ceramic or glass part is absolutely nondeformable.

In practice it is vital to control the width of the coalescence between the reinforcement and the parent metal c_n with the known joint compression to dimension b. This is possible if all the mutually related geometrical relations of the deformed wire are known. If the width of the coalescence of the individual wire with the parent metal is known, the mechanical properties of the reinforced brazed joint can be estimated in advance.

2 MODELS

In the field of welding, there are numerous mathematical, statistical, and physical-chemical models describing welding processes. A number of different approaches and methods are known for preparing models, but in practice two of them are preferred, i. e., the statistical one and the physical one. In engineering metallurgy, models for the calculation of forces and stresses in deformation are known.

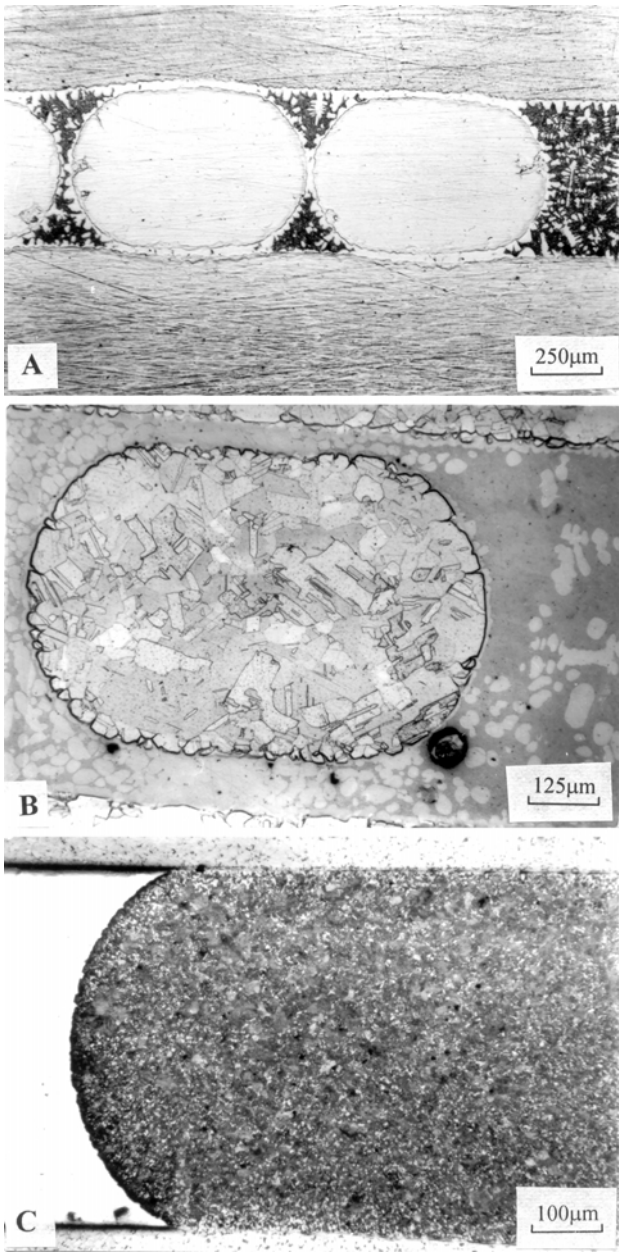

Figure 2: Flattened wires of the reinforcement in a reinforced brazed joint (A – brazing material: BNi-7, reinforcement and parent metal: austenitic steel AISI 304, $h/b \approx 0.36$; B – brazing material: BCuP-2, reinforcement and parent metal: copper, $h/b \approx 0.33$; C – brazing material: BAg-5, reinforcement: steel with 0.7 % carbon, parent metal: steel with 0.16 % carbon, $h/b \approx 0.28$)
Slika 2: Sploščene žice armature v armiranem spajkanem spoju (A – spajka: BNi-7, armatura in osnovni material: avstenitno jeklo AISI 304, $h/b \approx 0{,}36$; B – spajka: BCuP-2, armatura in osnovni material: baker, $h/b \approx 0{,}33$; C – spajka: BAg-5, armatura: jeklo z 0,7 % ogljika, osnovni material: jeklo z 0,16 % ogljika, $h/b \approx 0{,}28$)

In our case, the geometrical relationship between the deformed wire and the known compression is of primary importance since the mechanical properties of the reinforced brazed joint can be controlled. In the literature, such an approach has not yet been found.

Geometrical models were prepared on the basis of the following assumptions:

- the cross-section S of a circle is the S of a flat profile,
- during compression the wires only flatten and do not elongate; this is the actual state due to a much greater wire length l in comparison to its diameter d ($l/d >> 1$),
- only the wires, and not the parent metal, will deform.

Figure 3 shows the deformation of a round wire into a flat profile. The active bearing cross-section of each wire in the joint, S_1, is the rectangular part determined by flattening c_n and the height b of the profile, which is equal to the joint width. The inactive parts of the flat profile are the rounded ends, S_2. During wire compression the bearing cross-section S_1 transforms from an upright rectangle ($c_n < b$) through a square ($c_n = b$) into a lying rectangle ($c_n > b$, in the case of strong compression: $c_n >> b$). With the increase in c_n the bearing cross-section S_1 increases too at the expense of the inactive part S_2. In other words, the inactive cross-section of the round wire S may transform, by means of a strong compression, into the active cross-section $S_1 \approx S$.

The experimental results obtained with the reinforced joints (**Figure 2**) in copper and different steels show that the area S_2 has a shape similar to a segment but very rarely to a semicircle. This is to say that the rounding-off radius is greater than $b/2$, and the area S_2 is smaller than a semicircle with the radius of $b/2$. The area S_2 is presumably semicircular only at the beginning of compression when $c_n << b$. A similar shape is also obtained in the case when a square wire is compressed [7,8].

Several models of the deformation of the round-wire cross-section into a flat profile were prepared, i. e.,

- a model with a semicircular area S_2 (model index: n = 1),
- a model of a rectangle (model index: n = 2),
- a model with a segment area S_2 (model index: n = 3),
- a model with a parabolic ending of the area S_2 (model index: n = 4),
- an empirical mathematical model (model index: n = 5).

2.1. Model with a semicircular area S_2

The model is simple and represents a boundary condition with regard to the segment. With the compression of the wire and the joint, respectively, from d to b a semicircle always has a larger area S_2 than a segment, which gives the smallest width c_1 and the largest width a_1. On the basis of **Figure 3** it can be stated:

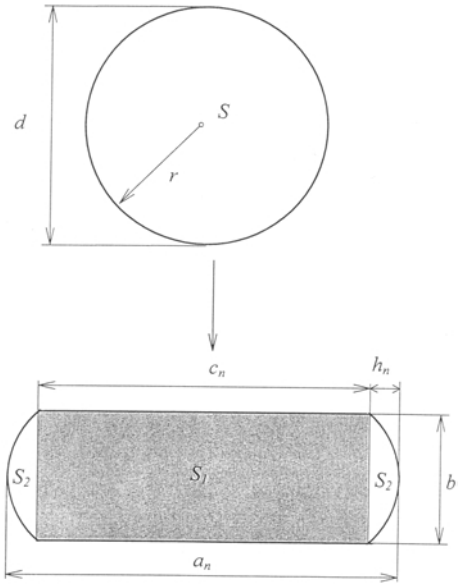

Figure 3: Geometrical relations between the circle and the flat profile (n = model index)
Slika 3: Geometrijsko razmerje med krogom in ploščatim profilom (n = indeks modela)

$$S = S_1 + 2S_2\,;\; h_n = h_1 = \frac{b}{2}$$

From this it is obtained:

$$c_n = c_1 = \frac{\pi}{4b}(d^2 - b^2) = \frac{\pi d^2}{4b} - 0.785b \tag{1}$$

$$a_n = a_1 = c_1 + b = \frac{\pi d^2}{4b} + 0.215b \tag{2}$$

2.2 Model of a rectangle

The model is unreal with regard to the actual state, but it represents another boundary condition with regard to the segment. In the compression of the wire and the joint, respectively, from d to b we have only the rectangular bearing cross-section S_1, which gives the largest width c_2. The model gets more real with a very strong compression when $c_2 >> b$. On the basis of **Figure 3** it can be stated:

$$S = S_1\,;\; h_n = h_2 = 0$$

From this it is obtained:

$$c_n = c_2 = \frac{\pi d^2}{4b} \tag{3}$$

$$a_n = a_2 = c_2 \tag{4}$$

2.3 Model with a segment area S_2

According to reference [9] and **Figure 4** the approximate calculation of the segment area S_2 equals

$$S_2 = \frac{h_3}{15}(6b + 8t) \tag{5}$$

and

$$t = \sqrt{\left(\frac{b}{2}\right)^2 + h_3^2} \tag{6}$$

The approximate formula of the segment area S_2 does not depend on the radius of the relevant circle R and the angle φ, which both determine the length of the segment arc (see **Figure 5**). Both parameters are the unknown and are difficult to choose optionally. The unknown width of protuberance h_3 is easier to determine since it varies between $0 < h_3 < b/2$ (half-height of the profile and half-width of the joint respectively). On the basis of Figure 3, the area of the flat profile in **Figure 4** is:

$$S = 2 \cdot \frac{S_1}{2} + 2S_2$$

By taking into account Eq. (6) and Eq. (5) it is found that the total width of flattening is

$$c_n = c_3 = \frac{\pi d^2}{4b} - \frac{2h_3}{15b}\left[6b + 8 \cdot \sqrt{\left(\frac{b}{2}\right)^2 + h_3^2}\right] \tag{7}$$

$$a_n = a_3 = c_3 + 2h_3 \tag{8}$$

With the selected dimensions h_3 in the above given range, a number of curves for c_3 are obtained. They vary between c_1 (item 2.1) and c_2 (item 2.2). Eq. (7) indicates that in selecting $h_3 = 0$ flattening $c_3 = c_2$ is obtained, which is the model of a rectangle. In selecting $h_3 = b/2$, however, a model with a semicircular area is obtained, which is hard to observe directly due to the approximate segment area (Eq. (5)). But it is valid if $h_3 = b/2$ is inserted into the area S_2 (from Eqs. (5), (6), and **Figure 4**) and if a real number is inserted for b. From this it is found that the double area S_2 equals the area of the circle with a diameter b, which makes a model with a semi-circular area:

$$2S_2 = 2 \cdot \frac{\left(\frac{b}{2}\right)}{15}\left(6b + 8 \cdot \sqrt{\frac{b^2}{2}}\right) \approx \frac{\pi b^2}{4}$$

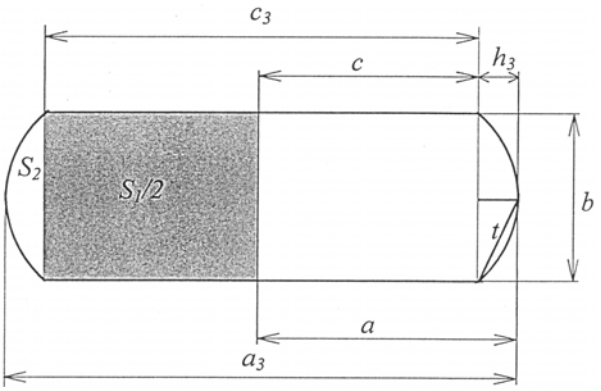

Figure 4: Model of the flat profile with a segment
Slika 4: Model ploščatega profila s krožnim odsekom

2.4 Model with a parabolic ending of the area S_2

The model was prepared on the basis of **Figure 5** with a sector. The flat-profile cross-section S consists of three partial areas, i.e.:

- S_1 – area of the rectangle between the two centres of the circles O_1 and O_2
- S_2 – area of four right-angled triangles between the sector and the rectangle
- S_3 – area of the two sectors.

The cross-section of the flat profile is equal to $S = S_1 + S_2 + S_3$.

$$S = 4b_4(a - R) + 2b_4\sqrt{R^2 - b_4^2} + 2R^2 \arcsin\frac{b_4}{R} \tag{9}$$

The cross-section of the flat profile can also be expressed as

$$S = 4ab_4 - b_4^2 f(x) \tag{10}$$

With the theorem of altitude, which indicates the relationship between the altitude and the longest side of a right-angled triangle, in accordance with **Figure 5** (below), R and, consequently, x are expressed as functions of a, c, and b_4.

If x is treated by the half-angle tangent formula (universal substitution), the expression $\tan\alpha = a - c/b_4$ is obtained, where α is the angle between the half-altitude of the compressed wire and the half of its arc (**Figure 5**). If instead of function f a new function g taking into account this dependence is used, we get:

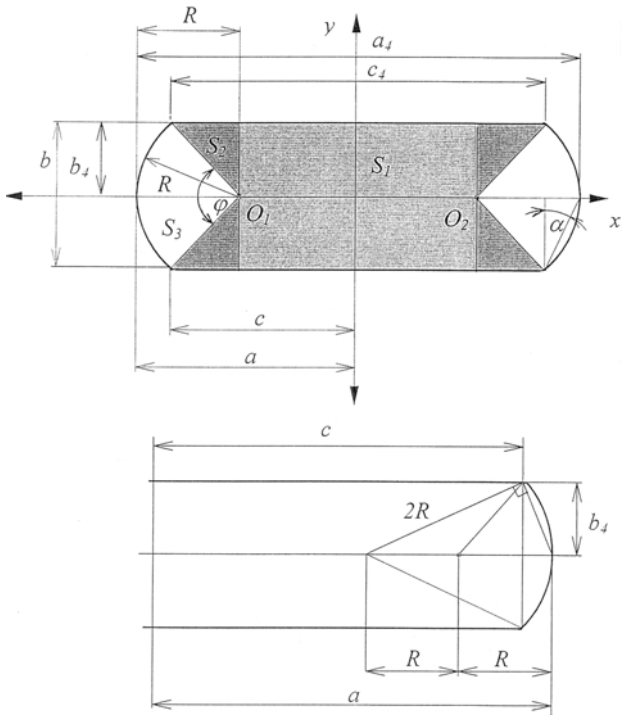

Figure 5: Model of the flat profile with a sector being a basis for a parabolic rounding
Slika 5: Model ploščatega profila z izsekom, ki jeosnova za parabolično zaokrožitev

$$S = 4ab_4 - b_4^2\, g\left(\frac{a-c}{b_4}\right) \tag{11}$$

The selected function g is defined by the equation $g(\tan\alpha) = f(\sin 2\alpha)$ and takes the following form:

$$g(u) = \frac{1+3u^2}{u} - \left(\frac{1+u^2}{u}\right)^2 \arctan u \tag{12}$$

When approximating this function we take the new function:

$$g(\xi) \approx \beta + \gamma\xi + \delta\xi^2$$

and require a minimum of the integral

$$\int_0^1 \left(\beta + \gamma\xi + \delta\xi^2 - g(\xi)\right)^2 d\xi$$

By minimizing the integral using the method of least squares, coefficients β, γ, δ can be calculated:

$\beta \cong -0.0207023$, $\gamma \cong 1.5924766$, $\delta \cong -0.6956118$

A quadratic approximation to the fundamental equation is:

$$S = 4ab_4 - b_4^2\left[\beta + \gamma\left(\frac{a-c}{b_4}\right) + \delta\left(\frac{a-c}{b_4}\right)^2\right] \tag{13}$$

By solving Eq. (13) and taking into account the total dimensions of the flattened wire, the final equations of the profile widths a_4 and c_4 are obtained:

$$a_n = a_4 = \frac{-(\gamma^2 - 4\beta\delta)\frac{b^2}{4} + \delta\pi d^2}{4\delta b} = \frac{\pi d^2}{4b} + 0.223b \tag{14}$$

$$c_n = c_4 = a_4 + \frac{\gamma b}{2\delta} = \frac{\pi d^2}{4b} - 0.92b \tag{15}$$

It is evident that a very complicated method provides a similar result to the model with a semicircular area. If a different function g was selected, the coefficients β, γ, and δ would change and a different result would be obtained. The method allows a free choice of the form of function g. It turned out that the equation obtained for c_4 was the basis of a simple calculation of the active bearing profile width that can replace all the previously shown models.

2.5 Empirical mathematical model

The model is based on the model with a parabolic end surface S_2 (item 2.4). In Eq. (15) $\gamma/2\delta$ is a constant with a value of –1.144659. Equation (15) can be written in a general form

$$c_n = c_5 = a_4 - k \cdot b; \quad 0.223 \le k \le 1.01 \tag{16}$$

where b is the profile height. The range of constant k, which was determined with the method of "trial and error", was compared with other models. It was found that with $k = 0.223$ the model of a rectangle is obtained, and with $k = 1.01$ the model of a semicircle is the result. The constant k ranging between these two values gives the model of a segment. Equation (16) can describe all the models presented, yet only for the profile width c_n. This is because the model is not based on a geometrical equality of the initial wire and profile cross-sections. Taking into account that for a synthesis of the reinforced brazed joint and its carrying capacity only the smaller profile width c_n is of importance, Eq. (16), with the corresponding Eq. (14), satisfies the needs of designing the reinforced brazed joint.

3 RESULTS AND DISCUSSION

A comparison of the models was made by calculations of the compression of the round cross-section wires with 1.0 mm and 0.7 mm diameters. The results obtained are shown in **Figures 6, 7, 8, and 9**.

The unreal and most simple geometrical model of the rectangle is getting more and more real with a stronger wire compression. With all the other geometrical models, with a stronger compression the ratio between the smaller profile width and the greater profile width heads towards 1, i.e., $c_n/a_n \rightarrow 1$ (**Figure 8**). That is to say that the other models approximate the model of the rectangle. For example, when flattening a 1.0 mm wire compressed to a profile height b of 0.2 mm, the ratio c_n/a_n with other models amounts to 0.94–0.98.

The important smallest width of wire flattening c_n, which determines the coalescence width of the flattened reinforcement wires and the parent metal in a reinforced brazed joint, offers the model of a parabola, and the greatest width the model of a rectangle. The greatest width of wire flattening a_n offers the model of a parabola, and the smallest width a_n the model of a rectangle. Consequently, the model of a parabola shows the lowest ratios c_n/a_n (**Figure 8**) and the highest ratio

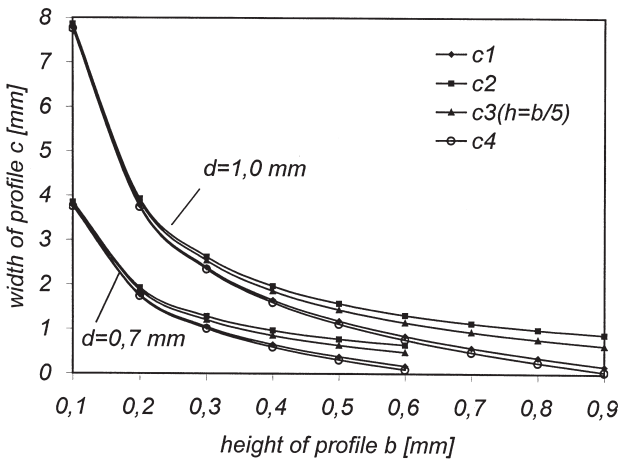

Figure 6: Width of wire flattening c_n (active bearing width of profile) as a function of wire compression to b (height of profile); 1, 2, 3, 4 – model indices

Slika 6: Širina sploščenja žice c_n (aktivna nosilna širina profila) kot funkcija stiskanja žice na b (višina profila); 1, 2, 3,4 – indeksi modelov

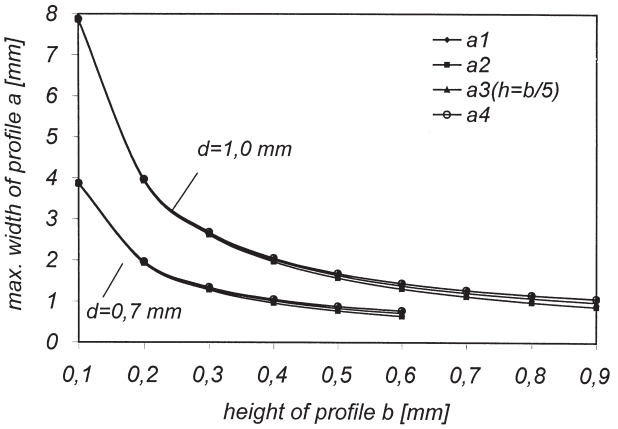

Figure 7: Width of wire flattening a (max. width of profile) as a function of wire compression to b (height of profile); 1, 2, 3, 4 – model indices

Slika 7: Širina sploščenja žice a (maksimalna širina profila) kot funkcija stiskanja žice na b (višina profila); 1, 2, 3,4 – indeksi modelov

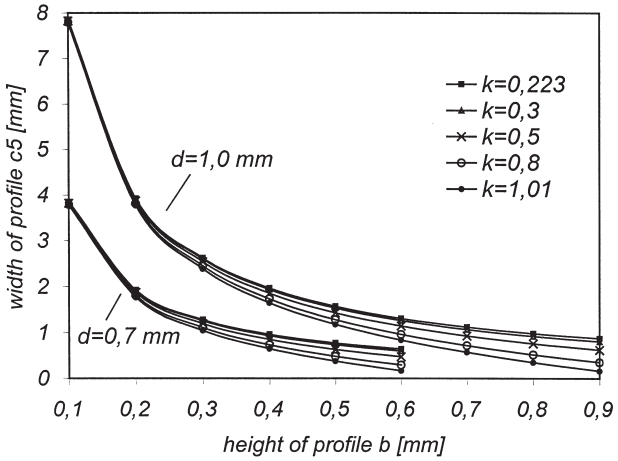

Figure 9: Width of wire flattening c_5 (width of profile) calculated using the empirical mathematical model

Slika 9: Širina sploščenja žice c_5 (širina profila), izračunana z uporabo empiričnega matematičnega modela

between the protuberance width and the profile height h_n/b. The ratio h_n/b is constant with all the models, regardless of the degree of flattening and the initial wire diameter. The ratio h_n/b amounts to 0 for the rectangle, to 0.2 for the segment $h_3 = b/5$, to 0.25 for the segment $h_3 = b/4$, to 0.33 for the segment $h_3 = b/3$, to 0.5 for the semicircle $h_1 = b/2$, and to 0.57 for the parabola.

The useless area of the flat profile S_2 is somewhat more pointed with the model of a parabola ($h_4/b > 0.5$), but at the same time it is the largest since the ratio c_n/a_n is the lowest.

The models differ in the profile width a_n much less than in the profile width c_n (**Figures 6 and 7**). For example, for the 1.0 mm wire the ratios a_2/a_4 between the model of a rectangle, which gives the smallest $a_n = a_2$, and the model of a parabola with the highest $a_n = a_4$ amount to 0.813 (with b = 0.9 mm), 0.934 (with b = 0.5 mm), and 0.989 (with b = 0.2 mm). There is almost no difference between $a_n = a_1$ (semicircular model) and $a_n = a_4$ (model of a parabola); therefore, the curves practically coincide. The ratios c_4/c_2 between the model of a parabola, which gives the smallest $c_n = c_4$, and the model of a rectangle with the highest $c_n = c_2$ amount to 0.049 (with b = 0.9 mm), 0.706 (with b = 0.5 mm), and 0.953 (with b = 0.2 mm). The model of a parabola is close to the model of the semicircle since the ratios c_4/c_1 amount to 0.833 (with b = 0.7 mm), 0.942 (with b = 0.5 mm), and 0.993 (with b = 0.2 mm). With little compression the model of a parabola differs significantly from the other models and gives very small values of $c_n = c_4$ (e.g., the ratio c_4/c_1 = 0.259 with b = 0.9 mm). Consequently, it is the least real in the first phase of compression.

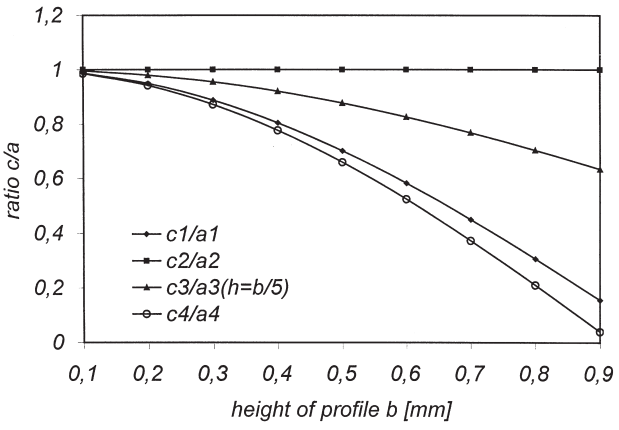

Figure 8: The ratio c/a as a function of wire compression to b (wire d = 1.0 mm); 1, 2, 3, 4 – model indices

Slika 8: Razmerje c/a kot funkcija stiskanja žice na b (žica d = 1,0 mm); 1, 2, 3,4 – indeksi modelov

For the calculation and control of the profile width c_n, an empirical-mathematical equation can substitute for all the geometrical models (**Figure 9**). The situation is practically the same as in **Figure 6**. The width c_5 is calculated from a_4 (model of a parabola) because, according to the model of a parabola, the dimension a is calculated independently from the dimension c, which is, however, not the case with the other models. With the other models, first c is calculated and from this it is possible to calculate dimension a.

The differences between the models obtained with weak compression reduce significantly with strong compression. With the mathematical models the ratio h_n/b is constant, regardless of the degree of wire compression. Experimental measurements showed different ratios h_n/b, i.e. ranging between 0.20 and 0.48, depending on the degree of flattening. The latter are in the range of the models presented.

The main cause should be looked for in different conditions (temperature, rate of deformation, friction) of wire flattening due to the use of different brazing materials having different melting points. Differing materials are also prone to flow differently under the same conditions. It is known that the deformation at high

temperatures is more continuous, which indicates that a metal will deform in a similar way as a very viscous substance. It is known too that the resistance to deformation increases with a higher rate of deformation and a decrease in the temperature.

During the formation of the reinforced brazed joint some of these parameters were not controlled because interest was focused on the influence of the coalescence of the reinforcement and the parent metal on the mechanical properties of the brazed joint. The deformability of the wires being compressed became the focus of our attention when a question was raised as to whether it is possible to predict the width of the coalescence c_n between the wire and the parent metal. Consequently, the above-mentioned models were prepared. Hopefully, the validity of one of the models in dependence of the parameters of wire deformability or a combination of the models with regard to the degree of wire flattening will be established.

4 CONCLUSIONS

The models for a round wire flattening into a flat profile by compression offer the basis for experimental studies to show which model gives the most realistic description of the practical situation. The boundary models and the least real ones are the models of a rectangle and that of a parabola. The models with the profile width a_n agree very well, while with the profile width c_n there are major differences, particularly in the first compression phase. The differences between the different models reduce if stronger compression is applied. Thus, all the models approximate the same point. All the geometrical models shown have a constant ratio between the protuberance width and the profile height h_n/b regardless of the degree of wire compression. Experimental studies will show whether this is really the case.

Because a round wire is compressed, the beginning of the compression process for the wire is best described by a model with a semicircular area S_2, whereas later on the model with a segment area S_2 is decisive since the experimentally obtained ratios between the protuberance width and the profile height h_n/b are < 0.5.

For an easy calculation of the profile width c_n an empirical mathematical model with the empirically selected constant k ranging between 0.223 and 1.01 was elaborated.

NOTATION

a maximum width of the profile
b height of the profile
c active bearing width of the profile
d wire diameter
h width of protuberance
k constant
l wire length
R radius of the sector with the model with a parabolic ending
S cross-sectional area of a circle and flat profile
S_1, S_2, S_3 partial cross-sectional areas of the flat profile
α angle between the half-altitude of the compressed wire and the half of its arc
β, γ, δ coefficients

ACKNOWLEDGEMENT

The author wish to thank to mag. Janez Barbič, univ. dipl. mat., for the help in the preparation of the model in Chapter 2.4.

5 REFERENCES

[1] Folley, G., Andrews, D. J. Joining ceramics to metals by brazing. In Proceedings of the 3rd Int. Conf. *on Brazing, High Temperature Brazing and Diffusion Welding*, DVS-Verlag GmbH, Düsseldorf, Aachen, 1992, 258–263

[2] Mirski, Z. Composite brazed joints with sintered carbides. In Proceedings of the 3rd International Conference *on Brazing, High Temperature Brazing and Diffusion Welding*, DVS-Verlag GmbH, Düsseldorf Aachen, 1992, 174–177

[3] Cao, J., Chung, D. D. L. Carbon fiber silver-copper brazing filler composites for brazing ceramics. *Weld. J.*, 71 (**1992**) 1, 21–24

[4] Suganuma, K. et al. New method for solid-state bonding between ceramics and metals. *J. Am. Ceram. Soc*, 66 (**1983**), 7, C117–C118

[5] Suganuma, K. et al. Effect of interlayers in ceramic-metal joints with thermal expansion mismatches. *J. Am. Ceram. Soc.*, 67 (**1984**) 12, C256–C257

[6] Zorc, B., Kosec, L. A new approach to improving the properties of brazed joints. *Welding Journal*, 79 (**2000**) 1, 24–31

[7] Klomp, J. T., Van de Ven, A. J. C. Parameters in solid-state bonding of metals to oxide materials and the adherence of bonds. *Journal of Materials Science*, 15 (**1980**) 10, 2483–2488

[8] Gubbels, G. H. M. et al. Aspects of the strength of nickel-silicon nitride joints. In Proceedings of 5th International Conference *on Joining of Ceramics, Glass and Metal*, DVS-Verlag GmbH, Düsseldorf, Jena, 1997, 133–137

[9] Bronštejn, J. N., Semendjajev, K. A. Matematični priročnik (Handbook of Mathematics), Tehniška založba Slovenije, Ljubljana 1997, 115 (in Slovene)